

## ***Influence of A-site cation size variation on the magnetic properties of a canted $RE_{0.7}Sr_{0.3}Fe_{0.9}Ni_{0.1}O_3$ ; (RE=rare earth) multiferroic system"***

***M. A. Ahmed<sup>a</sup>, N. Okasha<sup>b</sup>, S. M. Abdelwahab<sup>a</sup> and A. Abd Elazim<sup>c</sup>***

*a. Materials Science Lab. (1) Physics Department, Faculty of Science, Cairo University, Giza, Egypt.*

*b. Physics Department, Faculty of Girls, Ain Shams University, Cairo, Egypt.*

*c. Basic Science Department, Nahda University, Faculty of Engineering, Beni Suef, Egypt.*

### **Corresponding author:**

**Corresponding author: N. Okasha; [naokmo@yahoo.com](mailto:naokmo@yahoo.com)**

**Physics Department, Faculty of Girls, Ain Shams University, Cairo, Egypt**

**Tel, Fax no: 02035693738**

**Country code: 11722**

---

### ***Abstract***

The structural and magnetic properties of a series of orthoferrites,  $RE_{0.7}Sr_{0.3}Fe_{0.9}Ni_{0.1}O_3$ ; RE= La, Pr, Nd, Gd, and Dy were successfully prepared by the citrate-nitrate autocombustion method. All samples were antiferromagnetic with a weak ferromagnetic component due to small canting of the  $Fe^{3+}$  moments. The correlation between magnetic transition and structural distortion is discussed on the basis of the variation of the Néel temperature and the tolerance factor as a function of different ionic radii of the rare earth elements. The results reveal that, X-ray diffraction (XRD) analysis indicated that all samples crystallized in pure orthorhombic perovskite structure with space group Pbnm. The Goldschmidt tolerance factor for the perovskite decreases from 0.85 for  $La_{0.7}Sr_{0.3}Ni_{0.1}Fe_{0.9}O_3$  to 0.82 for  $Dy_{0.7}Sr_{0.3}Fe_{0.9}Ni_{0.1}O_3$  confirming that the crystal structure is orthorhombic. The molar magnetic susceptibility increased from 0.086 to  $emu\ g^{-1}\ mol$  at  $La^{3+}$  to 0.379  $emu\ g^{-1}\ mol$  at  $Dy^{3+}$  and the coercive field ( $H_C$ ) of the samples was increased from 129.38Oe for  $La_{0.7}Sr_{0.3}Ni_{0.1}Fe_{0.9}O_3$  to 164.15Oe for the  $Dy^{3+}$  substituted sample. The Néel temperature indicates the highest value (834K) at  $Dy^{3+}$ .

**Keywords;** Rare earth elements; Magnetic Properties; Orthoferrite; Antiferromagnet.

---

### ***1. Introduction***

Recently, a lot of interest was focused on the processing and characterization of mixed oxide ceramic powders [1–3]. Rare earth orthoferrite  $RFeO_3$  perovskite type oxides are of practical interest for electroceramic applications due to their attractive mixed conductivity displaying ionic and electronic defects. The importance of these materials is mainly due to their wide variety of applications in catalysis [4]. They can be used as an active catalyst for oxidation or reduction of pollutant gases [5,6] and as electrode materials in solid oxide fuel cell [7–9] or materials for technological chemical sensors as well as the detection of humidity, alcohol, gases [10,11] and oxygen permeating membranes. Magnetic ordering can make these sites inequivalent and give rise to four distinct Fe sublattices [12]. Orthoferrites are canted antiferromagnets with high transition temperature that monotonically decreased as the rare earth atomic number increases [13]. The ideal perovskite structure is cubic; the distortion of the perovskites from the cubic symmetry is measured by the so-called tolerance factor ( $t$ ) [14] and expressed as:

$$t = \frac{R_o + R_A}{\sqrt{2}(R_o + R_B)} \quad (1)$$

Where  $R_A$ ,  $R_B$  and  $R_o$  are the ionic radii of A site cation with coordination number 12, B site cation with coordination number 6 and oxygen anion with coordination number 6, respectively. This formula can be modified to determine the tolerance factor of a complex perovskite by substituting the average radius of two or more different cations. The tolerance factor of an ideal cubic perovskite is equal to 1. If the tolerance factor deviates from 1, structural distortions can occur. If  $t < 1$ , the A site cation is too small for its site, which results in  $BO_6$  octahedral tilting. Tilting of the  $BO_6$  octahedra within the perovskite structure leads to lowering its symmetry. Various types of possible tilting in perovskite are discussed as; if the tolerance factor is too small, corner shared perovskite structure is not stable. The tolerance factor range in which perovskite structure is preferred is 1.04–0.87.

In the present study, we substituted different rare earth for  $RE_{0.7}Sr_{0.3}Fe_{0.9}Ni_{0.1}O_3$ ; RE= La, Pr, Nd, Gd and Dy to influence the effect of rare earth cations radii on the crystal structure, microstructure, and magnetic properties of the investigated nanomultiferroics to optimum the condition which may be one of the major challenges for applications. Also one of our goals is to reach a optimum rare earth element, at which an improvement of the mentioned properties takes place. At such different ionic radii, one expects that the samples will be more applicable in the daily life.

## 2. Experimental technique

Multiferroic  $RE_{0.7}Sr_{0.3}Fe_{0.9}Ni_{0.1}O_3$ ; RE= La, Pr, Nd, Gd, and Dy were successfully prepared by the citrate-nitrate autocombustion method [15, 16]. The molar ratio of metal nitrates to citric acid was 1: 1. A small amount of ammonia was added to the solution to adjust the pH value at 7. The precursor mixture was then heated to allow evaporation and to obtain a dried product in the form of uniformly colored gray fibers containing all the cations homogeneously mixed together at the atomic level. After cooling to room temperature it was grinded properly for half an hour in an agate mortar. The powder was characterized by X-ray diffraction to assure of the formation of the multiferroic in single phase without any impurity. Crystal structure and lattice parameters of the synthesized nanostructures were determined by X-ray diffraction technique; (Proke DS) with Cu  $K_\alpha$  radiation source ( $\lambda = 1.5418\text{\AA}$ ). The average crystallite size (L) of nanometric orthoferrite was calculated using the Debye-Scherrer's formula [19];  $L = 0.89\lambda/\beta \cos\theta$ , where  $\lambda$  is the wavelength of X-ray,  $\theta$  is the angle of reflection and  $\beta$  is the FWHM. High resolution transmission electron microscope (HRTEM) model (JEOL-1010) was used for studying the morphology of the nanostructures and their particle size. HRTEM is one the most powerful tools to image the nanostructure materials down to atomic resolution to correlate their chemical and physical properties. The dc magnetic susceptibility measurements were carried out using Gouy's method and at different temperatures ranging from 295K up to 950K as a function of applied magnetic field using different magnetic field intensities 1100, 1300 and 1660 Oe. The temperature of the samples was measured using K- type thermocouple with junction near the sample keeping it free. The accuracy of magnetic susceptibility measurements was  $\pm 1\%$  and the data was reproducible. The hysteresis and magnetization measurements were performed using vibrating sample magnetometer

(VSM; 9600 – 1LDJ; USA) with a maximum applied field of nearly 20kOe at room temperature. The magnetoelectric coefficient was measured for all prepared samples.

### 3. Results and Discussion:

#### 3.1 X-ray analysis:

The Phase identification and structural analysis due to X-ray diffraction patterns of the multiferroic samples  $RE_{0.7}Sr_{0.3}Fe_{0.9}Ni_{0.1}O_3$ ; RE= La, Pr, Nd, Gd, and Dy were shown in Fig.(1:a,b). it is reveals that, all the samples are found to be single-phase perovskite orthorhombic structure with space group  $Pnma$  and no spurious phases are observed indicate that, the formation of solid solution can eradicate unfavorable phases. These contradictory results may be due to the influence of the oxygen stoichiometry on the phase formation. All planes in XRD charts of the samples were compared and indexed with ICDD card No.(04-007-9985) while for  $La^{3+}$  was compared with ICDD card No. 01-089-1269. The broad XRD peaks confirm that the samples are in nanocrystalline form. The lattice parameters a, b and c were calculated on the basis of the orthorhombic unit cell and reported in Table (1).

Table (1): Values of the lattice parameters (a, b and c), unit cell volume, crystallite size, and tolerance factor for  $RE_{0.7}Sr_{0.3}Fe_{0.9}Ni_{0.1}O_3$ ; RE=La, Pr, Nd, Gd, and Dy nanomultiferroics.

RE ions	R(nm)	a(Å)	b(Å)	c(Å)	V(Å <sup>3</sup> )	Crystallite size (L) XRD nm	Particle size (L) HRTEM nm	Tolerance factor(t)
La	1.216	6.663	7.935	8.977	474.622	34	22	0.851
Pr	1.179	6.535	7.455	8.356	407.091	35	13	0.843
Nd	1.163	6.495	7.123	8.145	376.819	32	23	0.839
Gd	1.107	6.289	7.051	7.985	354.084	34	29	0.826
Dy	1.083	6.088	6.995	7.609	324.033	27	40	0.820

From Figure (2a) and Table (1) it seen that, the lattice parameters decreases with decrease the ionic radii were found to expand marginally with the inclusion of high ionic radius of RE as ( $La^{3+}$  ion). Because of larger ionic size of  $RE^{3+}$  ions compared to that of  $Fe^{3+}$ , a small distortions in the lattice due to  $RE^{3+}$  substitutions were observed also due to changes in the  $Fe^{3+}(R^{3+})-O-Fe^{3+}$  and  $R^{3+}-O-Ni^{2+}$  bond angles and  $Fe^{2+}/Ni^{2+}-O$  bond lengths, from those of  $NiO.Fe_2O_3$ . The tolerance factor (t) for the investigated samples was calculated from the relation (1). The values of the tolerance factor as shown in Fig (2b) and Table (1) indicate that, the orthorhombic structure for the samples of  $RE_{0.7}Sr_{0.3}Fe_{0.9}Ni_{0.1}O_3$ ; RE= La, Pr, Nd, Gd and Dy because of the radii of  $RE^{3+}$  and  $Sr^{2+}$  were taken in 9-fold coordination [17] while that for Fe and Ni were 0.85 indicated the orthorhombic structure of the investigated perovskite samples agree well with the data obtained from XRD analysis as mentioned above. By decreasing radii of the rare earth cation from  $La^{3+}$  to  $Dy^{3+}$ , the tolerance factor decreases due to the difference in the ionic radii between the A site  $RE^{3+}$  cations . The decrease in the tolerance factor means that

the distortion increases. This distortion originated from tilting of  $(\text{FeO}_6)$  octahedron as a result of decreasing the  $R_A$  cation size as well as the Fe–O–Fe angle decreasing.

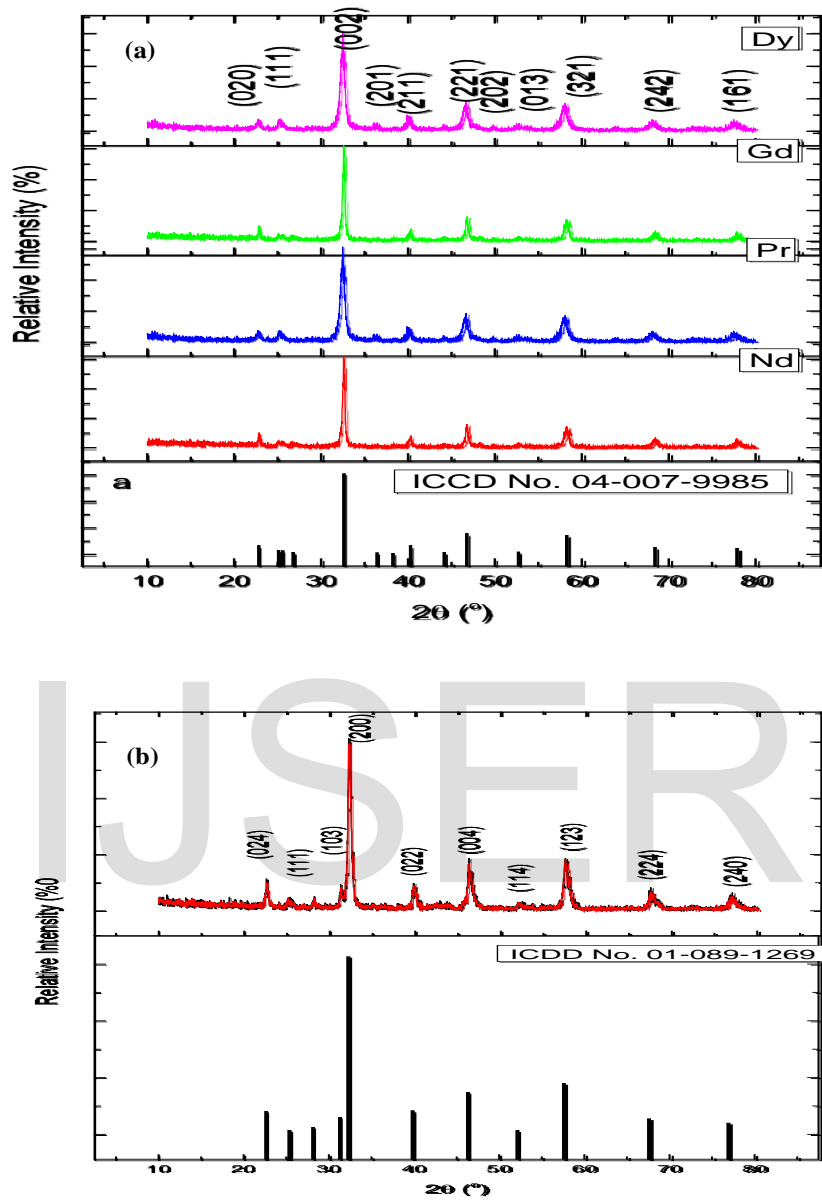


Fig. (1:a, b): XRD Diffraction patterns for  $\text{RE}_{0.7}\text{Sr}_{0.3}\text{Fe}_{0.9}\text{Ni}_{0.1}\text{O}_3$ ; RE= La, Pr, Nd, Gd, and Dy nanocrystalline samples.

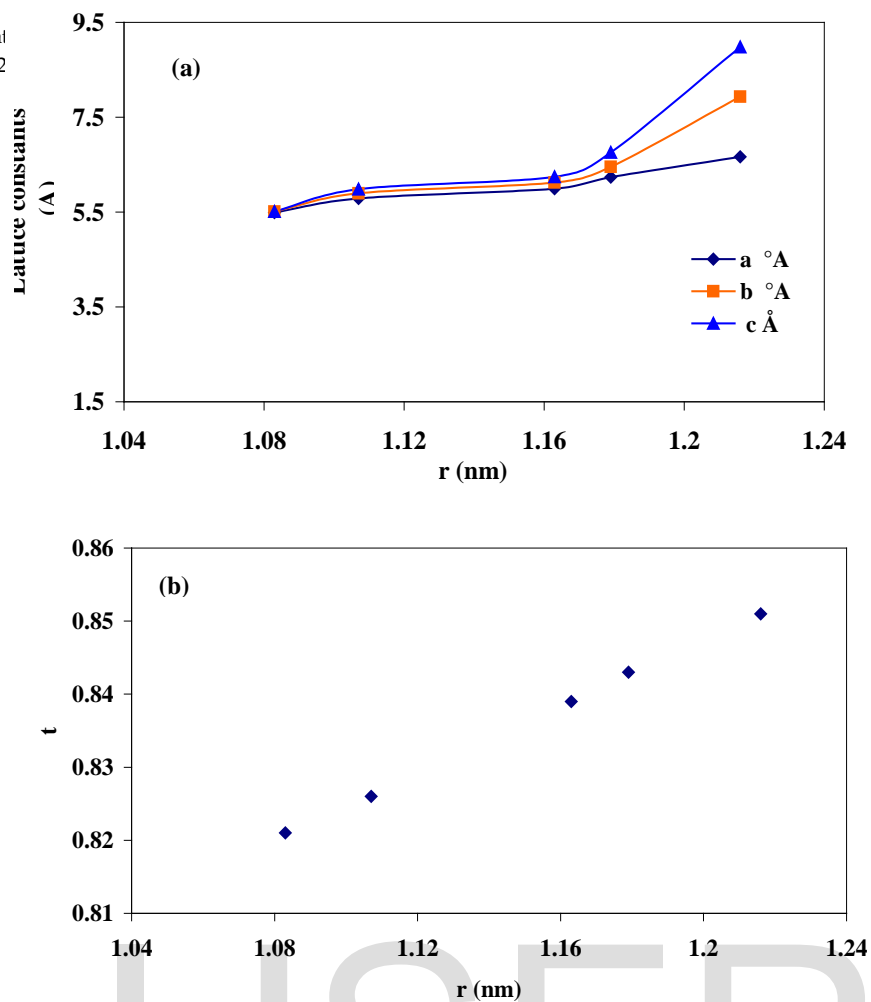


Fig. (2: a, b): a) Variation of lattice constants at different ionic radii. b) Effect of ionic radii on the Tolerance factor (t) for  $\text{RE}_{0.7}\text{Sr}_{0.3}\text{Fe}_{0.9}\text{Ni}_{0.1}\text{O}_3$ ; RE= La, Pr, Nd, Gd, and Dy.

### 3.2. Microstructure and densification

Figure (3) shows high resolution transmission electron microscope (HRTEM) micrographs for studying the effect of  $\text{RE}^{3+}$  substitution on the crystallite size and shape of the  $\text{RE}_{0.7}\text{Sr}_{0.3}\text{Fe}_{0.9}\text{Ni}_{0.1}\text{O}_3$ ; RE= La, Pr, Nd, Gd, and Dy nanomultiferroic samples. The data in the Figure clarified that, the particles were seen in clear platelet form and crystallized in small nanoparticles ranged from 22-30 nm as reported in Table (1). The clear images could be mainly due to the formation of single domain rather than multidomain and agglomerated particles appeared due to relatively large magnetization for these small particles.

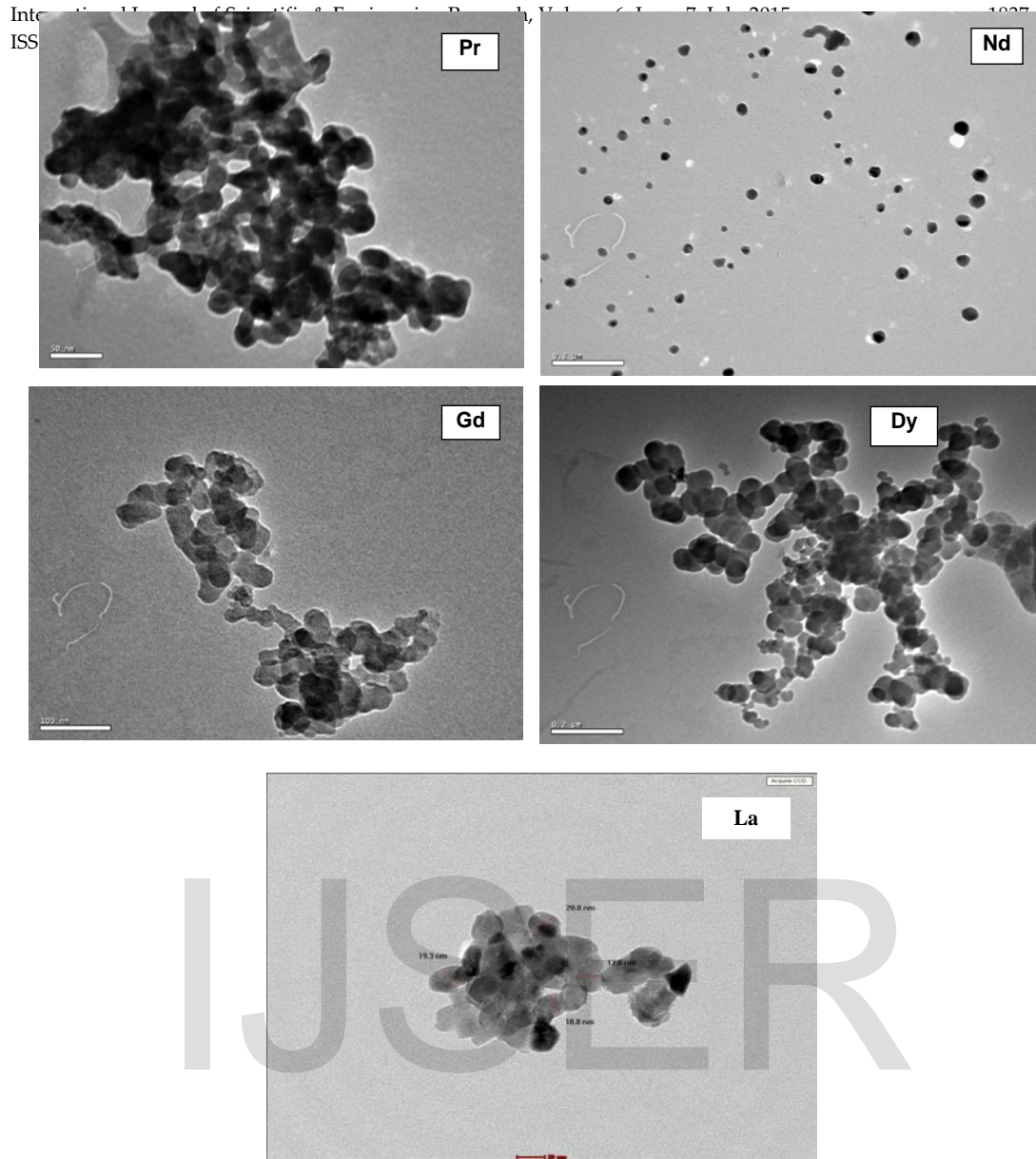


Fig. (3): HRTEM morphology for  $\text{RE}_{0.7}\text{Sr}_{0.3}\text{Fe}_{0.9}\text{Ni}_{0.1}\text{O}_3$  nanomultiferroics system doped rare earths;  $\text{La}^{3+}$ ,  $\text{Pr}^{3+}$ ,  $\text{Nd}^{3+}$ ,  $\text{Gd}^{3+}$ , and  $\text{Dy}^{3+}$  ions.

### 3.3 Magnetic properties:

The temperature dependence of the magnetic susceptibility ( $\chi_M$ ) as a function of applied magnetic field intensities of  $\text{RE}_{0.7}\text{Sr}_{0.3}\text{Fe}_{0.9}\text{Ni}_{0.1}\text{O}_3$ ; RE= La, Pr, Nd, Gd, and Dy nanomultiferroic samples is shown in Fig. (4a). It is clear that, the values of  $\chi_M$  decrease slowly with increasing the temperature until reaching the Néel temperature ( $T_N$ ). The general behavior of the samples before  $T_N$  is antiferromagnetic. The magnetic ordering of  $\text{Fe}^{3+}$  ions is that of a canted antiferromagnet of the G-type [18].

It is known that [18], The basic antiferromagnetic spin arrangement of  $\text{Fe}^{3+}$  ions along the a-axis is related to the magnetic symmetry of the configuration (G-type) and the ferromagnetic spin component along c-axis due to canting of  $\text{Fe}^{3+}$  spins. In other words, the substitution of  $\text{RE}^{3+}$  of different radius will change the bond angle of  $\text{Fe}^{3+}-\text{O}^{2-}-\text{Fe}^{3+}$ , which leads to the suppression of the spatially modulated spiral spin structure and hence the appearance of weak ferromagnetism. Moreover, the change in tolerance factor due to substitution of different  $\text{RE}^{3+}$  could be achieved by increasing exchange interaction between  $\text{Fe}^{3+}-\text{Fe}^{4+}$ , which could increase the canting angle of the antiferromagnetically ordered spins and give rise to an increase in magnetization for  $\text{Dy}^{3+}$  (2.87 emu/g). There is an improvement in the magnetic properties where the value of  $\chi_M$  increased from 0.086 emu/g. mole of the  $\text{La}^{3+}$  to 0.379 emu/g. mole of  $\text{Dy}^{3+}$  at 300K and 1100 Oe. From these data, one could argue that, the large improvement of the magnetization by rare earth cation substitution depends on the strength and type of exchange interaction and/or canting angle as well as buckling of the  $\langle \text{FeO}_6 \rangle$  octahedron. At lower temperature, the easy axis of magnetization begins to deviate towards the basal plane giving rise to the so-called spin reorientation process which always occurs at temperatures much lower than the Neél temperature of the orthoferrite. The difference in trend and values of  $\chi_M$  with the change of the rare

earth element depends on the following factors [19]:

- (i) The coordination number of the A site cation (rare earth).
- (ii) The ionic radius of the rare earth which affects directly on the calculated value of the tolerance factor.
- (iii) The atomic number of the rare earth element.
- (iv) The number of 4f electrons which in turns controls the value of the effective magnetic moment.

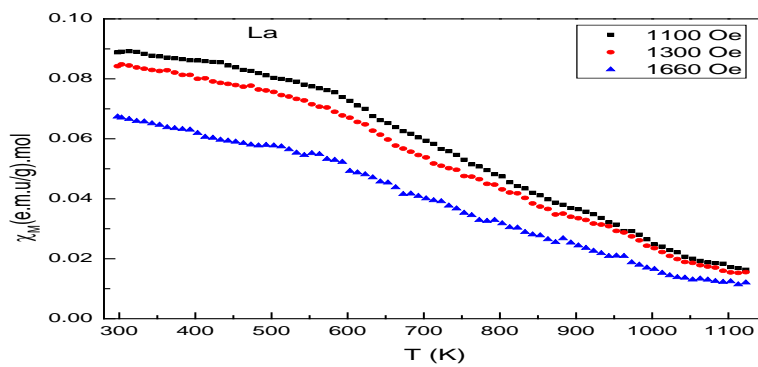
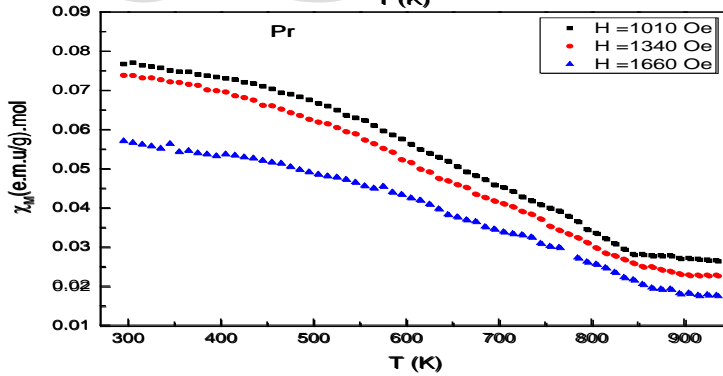
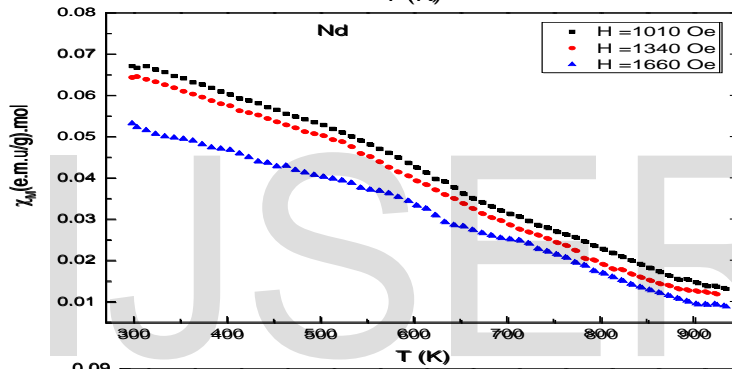
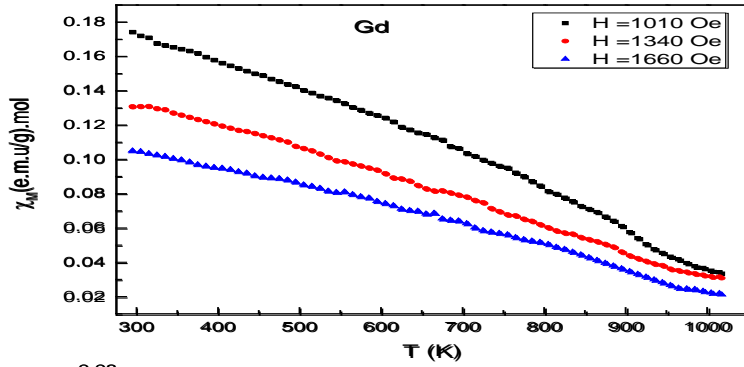
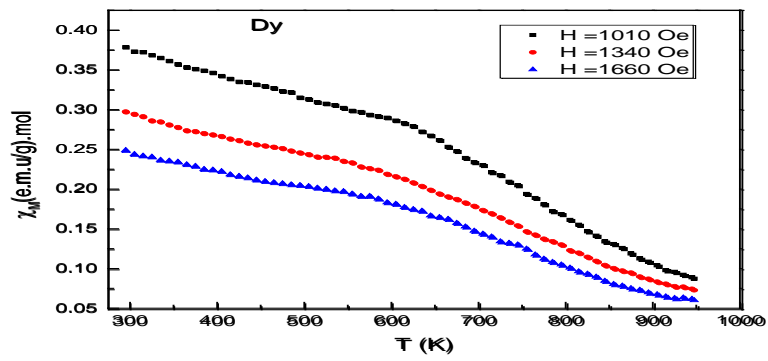




Fig. (4): Dependence of the molar magnetic susceptibility ( $\chi_M$ ) on the absolute temperature for  $RE_{0.7}Sr_{0.3}Fe_{0.9}Ni_{0.1}O_3$ ; RE= La, Pr, Nd, Gd, and Dy nanosamples

The dependence of  $T_N$  on rare earth radii is shown in Fig (4b) and reported in Table (2). The data show that,  $T_N$  decreases with increasing in radii up to  $Pr^{3+}$  after which it increases at  $La^{3+}$ .  $T_N$  generally reflects the strength of the superexchange interaction of the  $Fe^{3+}$  ions through the intervening of oxygen anions. The type of exchange interaction here is believed to be antiferromagnetic [20] and depends on the Fe–O–Fe distance as well as the buckling angle Fe–O–Fe. The  $RE^{3+}$  ions; in the present study; decreases the values of the tolerance factor; as reported in Table (1); which indicated lowering the value of the Fe–O–Fe angle [21] as well as induced distortion. This distortion in the  $(FeO_6)$  octahedron, i.e., the decrease in the buckling angle leads directly to a decrease in the Néel temperature. In other words, the decreasing in  $T_N$  is due to the replacement of smaller ionic radius ( $Dr^{3+} = 1.083\text{\AA}$ ) instead of the larger ionic radius ( $La^{3+} = 1.216\text{\AA}$ ). This agree well with the magnetic behavior due to formation of oxygen vacancies which could increase the canting angle of the antiferromagnetically ordered spins and give rise to an increase in magnetization as mentioned before.

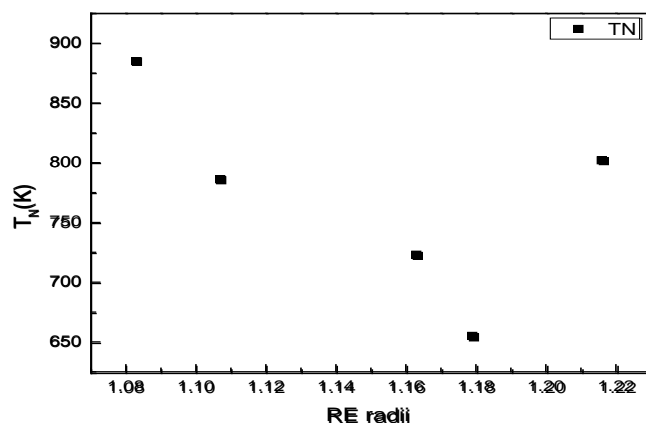


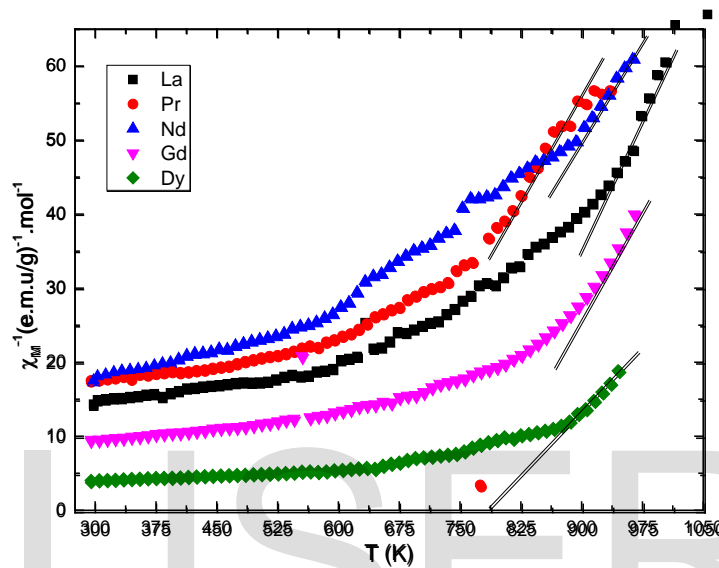
Fig. (5): The effect of rare earth radii on Néel temperature  $T_N$ .

The reciprocal of molar magnetic susceptibility is plotted with absolute temperature for all nanometric samples Fig. (6). The data obeys the well known Curie-Weiss law, where  $\chi_M$  varies linearly with temperature in the paramagnetic

region. The values of the Curie constant and the effective magnetic moment were calculated from

$$C = 1/\text{slope} \quad , \quad \mu_{\text{eff}} = 2.83\sqrt{C} \quad (2)$$

and  $\Theta$  is calculated from the intercept of the straight line with the temperature axis. The data are reported in table (2) where  $\Theta$  gives +ve values pointing to the weak ferromagnetic character for all investigated samples.



The room temperature magnetization field (M-H) curves with a maximum applied field of 2T for  $\text{RE}_{0.7}\text{Sr}_{0.3}\text{Fe}_{0.9}\text{Ni}_{0.1}\text{O}_3$ ; RE= La, Pr, Nd, Gd and Dy nanosamples are shown in Fig. (5). It is found that the hysteresis curves do not saturate. The remanent magnetization ( $M_r$ ) and magnetic coercive field ( $H_c$ ) of the investigated samples are summarized in Table (2).

Table (2): Values of the magnetic parameters; saturation magnetization ( $M_s$ ),

RE	Radii(Å)	$M_s$	$M_r$	$M_r/M_s$	$H_c(\text{Oe})$	$C(\text{emu/gmol k})$	$\Theta(\text{K})$	$\mu_{\text{eff}}(\text{B.M})$	$\chi_M$ (emu/gmol)
----	----------	-------	-------	-----------	------------------	------------------------	--------------------	--------------------------------	------------------------

remanence magnetization ( $M_r$ ), squareness ratio ( $M_r/M_s$ ), coercive field ( $H_c$ ), the magnetic constants, and Néel temperature ( $T_N$ )K for  $\text{RE}_{0.7}\text{Sr}_{0.3}\text{Fe}_{0.9}\text{Ni}_{0.1}\text{O}_3$ ; RE=La, Pr, Nd, Gd and Dy nanomultiferroics.

<b>La</b>	<b>1.216</b>	<b>0.0593</b>	<b>0.037</b>	<b>0.062</b>	<b>129.35</b>	<b>4.46</b>	<b>750</b>	<b>5.985</b>	<b>0.086</b>
<b>Pr</b>	<b>1.179</b>	<b>0.703</b>	<b>0.044</b>	<b>0.0624</b>	<b>133.5</b>	<b>5.61</b>	<b>622</b>	<b>6.707</b>	<b>0.078</b>
<b>Nd</b>	<b>1.163</b>	<b>0.814</b>	<b>0.068</b>	<b>0.0834</b>	<b>55404</b>	<b>3.36</b>	<b>664</b>	<b>5.405</b>	<b>0.079</b>
<b>Gd</b>	<b>1.107</b>	<b>1.772</b>	<b>0.079</b>	<b>0.0449</b>	<b>201.5</b>	<b>5.19</b>	<b>774</b>	<b>6.452</b>	<b>0.175</b>
<b>Dy</b>	<b>1.083</b>	<b>2.87</b>	<b>0.08</b>	<b>0.0278</b>	<b>113.2</b>	<b>9.81</b>	<b>784</b>	<b>8.874</b>	<b>0.379</b>

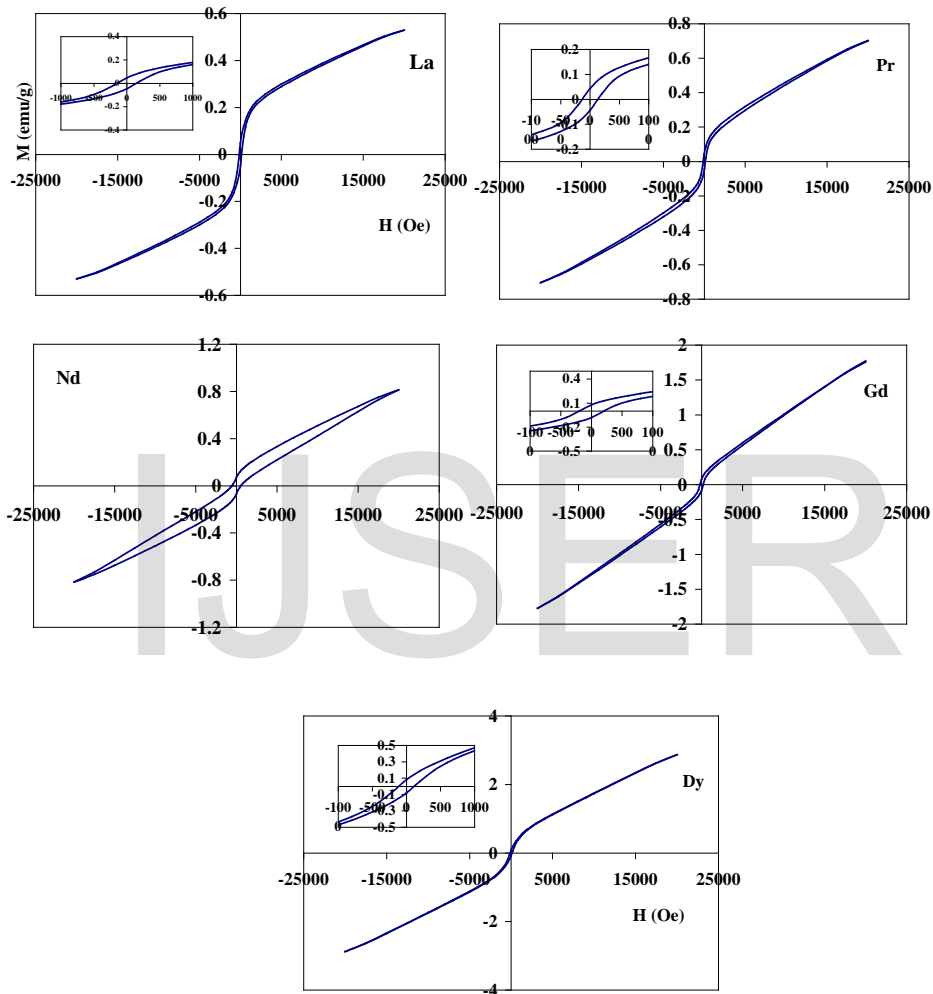


Fig. (5): Variation of hysteresis loops of  $\text{RE}_{0.7}\text{Sr}_{0.3}\text{Fe}_{0.9}\text{Ni}_{0.1}\text{O}_3$  nanomultiferroics at different doped rare earths;  $\text{La}^{3+}$ ,  $\text{Pr}^{3+}$ ,  $\text{Nd}^{3+}$ ,  $\text{Gd}^{3+}$ , and  $\text{Dy}^{3+}$  ions.

Compared to  $M_r$  value ( $0.062 \text{ emug}^{-1}$ ) of  $\text{La}^{3+}$  ( $0.08 \text{ emug}^{-1}$ ),  $M_r$  values of  $\text{Dy}^{3+}$  is highly in this study. This increase could be attributed to that A-site substitution by different rare earths which have different radii leads to enlarge the degree of

distortion, which leads to spontaneous magnetization [23] as well as increase in remanent magnetization as mentioned before. The large  $M_s$  and unsaturated M-H behavior of the solid solutions suggests their antiferromagnetic nature with weak ferromagnetism [22]. Moreover, the highest  $H_c$  value at  $Gd^{3+}$  ion (201.5 Oe) is due to the contribution from the large single ion anisotropy from the rare earth sublattice. Substitution of rare earth ion into the spinel structure has been reported to lead to structural distortion [24-26] and to induce strains in the material and significantly modify the magnetic properties.

#### **4. Conclusions**

1. Single phase  $RE_{0.7}Sr_{0.3}Fe_{0.9}Ni_{0.1}O_3$ ; RE= La, Pr, Nd, Gd, and Dy nanomultiferroic samples were successfully prepared using citrate autocombustion technique.
2. XRD analysis reveals orthorhombic distorted perovskite structure in all the investigated samples with rare-earth ions substitution where the lattice parameters reduces with decrease ionic radii of rare earth ions.
3. Both lattice parameters (a, b, and c) and tolerance factor decrease with decreasing ionic radius of  $RE^{3+}$  ions.
4. An enhanced magnetic moment was also observed for  $RE_{0.7}Sr_{0.3}Fe_{0.9}Ni_{0.1}O_3$ ; RE= La, Pr, Nd, Gd and Dy nanomultiferroics, attributed to the phase purity and also for the broken cycloid spins structure
5. Temperature and magnetic field dependent magnetization demonstrates the favorable effect of RE radii with huge enhanced magnetization.
6. There is an improvement in the magnetic properties where the value of  $\chi_M$  increased from 0.086 emu/g. mole of the  $La^{3+}$  to 0.379 emu/g. mole of  $Dy^{3+}$  ion.
7. La and Dy substituted samples suggests their use as pressure sensor at room temperature, chemical sensors as well as the detection of humidity, alcohol, gases and oxygen permeating membranes.

#### **5. Acknowledgments**

I would like to express my sincere gratitude to my dear advisor Prof. Dsc. Dr. M. A. Ahmed. It was his guidance and support that helped me through all the difficult time. I will surely benefit from his creative thoughts, suggestions and dedication throughout the rest of my life.

## 6. References

- [1] E.D. Wachsman, in: T. Hirai, S.I. Hirano, Y. Takeda (Eds.), *Progress in Ceramic Basic Science: Challenge Toward the 21st Century*, Ceramic Society of Japan, Tokyo, (1996) 129.
- [2] J.W. Stevenson, T.R. Armstrong, R.D. Carneim, L.R. Perderson, W.J. Weber, J. Electrochem. Soc. **143** (1996) 2722.
- [3] X. Liu, W. Zhong, S. Yang, Z. Yu, B. Gu, Y. Du, Phys. Stat. Sol. A **193** (2002) 314.
- [4] S. Ounnunkad, Solid State Commun. **138** (2006) 472.
- [5] Dabrowski B., Kolesnik S., Baszczuk A., Chmaissem O., Maxwell T., Mais J. "Structural, transport, and magnetic properties of RMnO<sub>3</sub> perovskites (R=La, Pr, Nd, Sm, 153Eu, Dy)" *Journal of Solid State Chemistry*, **178** (2005) 629.
- [6] S.Sankarajanb, K. Sakthipandi, V. Rajendran "Effect of Rare Earth Ions on Transition Temperature in Perovskite Materials by On-Line Ultrasonic Studies". *Materials Research*, **15** N4, (2012) 517.
- [7] W.J. Kuen, L.K. Pah, A.H. Shaari, C.S. Kien, N. Siau, W. and A. Gan Han Mingl "Effect of Rare Earth Elements Substitution in La site for LaMnO<sub>3</sub> Manganites". *Pertanika J. Sci. & Technol.*, **20**, №1, (2012) 81.
- [8] L.J.M.J. Blomen, M.N. Mugerwa, *Fuel Cell Systems*, Plenum, New York, (1993).
- [9] T. Yao, A. Ariyoshi, T. Inui, J. Am. Ceram. Soc. **80** (9) (1997) 2441.
- [10] T. Inone, N. Seki, K. Eguchi, H. Arai, J. Electrochem. Soc. **137** (1990) 2523.
- [11] L.B. Alcock, R.C. Doshi, Y. Shea, *Solid State Ionics* **51** (1992) 281.
- [12] T.M. Rearick, G.L. Catchen, J.M. Adams, *Phys. Rev.*, B **48** (1993) 224.
- [13] Luigi Sangaletti, Laura E. Depero, Brigida Allieri, Patrizia Nunziante, Enrico Traversa, J. Eur. Ceram. Soc. **21** (2001) 719.
- [14] G. Karlsson, *Electrochim. Acta* **30** (1985) 1555.
- [15] M. Ahmed, N. Okasha, S.I. Eldek, *Nanotechnology* **19** (2008) 065603.
- [16] M.A. Ahmed, S.I. El-Dek, A. Abd Elazim, superlattices and microstructures, **74** (2014) 34.
- [17] W.B. Li, H. Yoneyama, H. Tamura, *Nippon Kagaku Kaishi* **2** (1982) 761.

- [18] H. Falcon, A. E. Goeta, G. Punte, R. E. Carbonio, *J. Solid State Chemistry* **133** (1997) 379.
- [19] M.A. Ahmed, S.I. El-Dek, *Materials Letters* **60** (2006) 1437.
- [20] P. W. Anderson, *Phy. Rev.*, **79** (1950) 350-356 and 705.
- [21] S. Komornicki, L. Fournès, J. Grenier, F. Ménil, M. Pouchard, P. Hagenmuller, *Materials Research Bulletin*, **16** (1981) 967.
- [22] J.S. Kim, C.L. Cheon, Y.N. Choi, P.W. Jang, *J. Appl. Phys.* **93** (2003) 9263.
- [23] W.M. Zhu, Z.G. Ye, *Appl. Phys. Lett.* **89** (2006) 23-29.
- [24] Rezlescu N, E Rezlescu, The influence of Fe substitutions by R ions in a Ni-Zn Ferrite, *Solid State Communications* **88** ( 1993) 139-141.
- [25] Rezlescu N, E. Rezlescu, C. Pasnicu and M. L. Craus, Effect of rare earth ions on some properties of a nickel-zinc ferrite, *J. Phys.: Condens. Matter* **6** (1994) 5707-5716.
- [26] Fuxiang Cheng, Chunsheng Liao, Junfeng Kuang, Zhigang Xu, Chunhua Yan, Liangyao Chen, Haibin Zhao, and Zhu Liu, Nanostructure magneto-optical thin films of rare earth (RE=Gd, Tb, Dy) doped cobalt spinel by sol-gel synthesis, *J. Appl. Phys.*, **85** (1999) 2782-2784.

IJSER